Real-time probabelistic forecasts for the 2018 – 2019 Ebola outbreak in Northern Democratic Republic of Congo

CANDIDATE NUMBER2

September 10, 2019

Word count: XXXX

Abstract

Abstract

Contents

1 Introduction

Real time modelling of infectious diseases can play a crucial role during disease outbreaks like the ongoing Ebola outbreak in the north eastern Democratic Republic of Congo (DRC). During the previous large outbreak of Ebola in Western Africa in 2014–2015, many different models were developed[1] and used both to increase our understanding of the outbreak and to predict the spread of the outbreak. Estimates were used in official planning[**?**] and for example to estimate needed bed capacity [2]. Disease modelling has also been sucesfully implemented for for example Zika [3] and influeza [4] among many other diseases. To effectively use results from mathematical modelling in an outbreak it is of key importance that modelling outputs are integrated into the outbreak response and decision making [5]. This means that forecasts need to be availabel in real-time and be integrated into the outbreak surveillance information flow. In additionmproved communication and embedding of modelling and modellers into the outbreak response is needed.

For forecasts to be useful in an outbreak situation, the models need to incorporate uncertainty into the predictions[6, 7, 8]. Without understanding the range of possible outcomes from a model and their associated probabilities it is very difficult to support effective public health action in outbreak situations. Evaluting such probabelstic forecasts requires us to not just assess the accuracy of point predictions, but to assess if the model correctly assess it's own uncertainty. A model that that sucesfully asseses it's own uncertainty is calibrated. We should strive to create well calibrated models that can be updated in real-time and that that are interpretable and can be used in the outbreak response.

In this thesis, we will describe a framework for flexibly producing probabelistic forecasts and assess how well the resulting models can be used in the onogin Ebola outbreak in north-eastern DRC. We will compare different models to choose the best model and to explore the epidemiology of the current outbreak.

1.1 Ebola outbreak in North Kivu and Ituri provinces

On the 1st of August 2018, the minstry of health in the Democratic Republic notified the WHO about a new Ebola outbreak in the North Kivu province [9]. North Kivu is a populous region in north eastern DRC that borders both Rwada and Uganda. By the 27th of September the outbreak had continued spreading and the WHO assessed that the outbreak constiuted a very high national and regional risk[10].

Due to distrust from the local community the outbreak response has been challenging. This has lead to difficulty in tracing contracts, giving vaccinations and treating patients. There have been many episodes of violence directed towards the ebola responders which has led to fatalities and multiple stops in the response work[11, 12].

During the outbreak, the experimental vaccination rVSV-ZEBOV-GP has been used in a ring vaccination strategy. The vaccine was given under the compasionate use regime and have been evaluated during the outbreak. Preliminary data shows positive signs that this vaccine might provide some protection from Ebola [13]. been given to health-care workers and children. This outbreak has also seen a randomised trial for medicines to treat ebola. The trial was terminated at the 12th of August due to findings that two of the four drugs that were included showed clear effect of reducing mortaltiy from Ebola, especially with

early treatment [14] At the time of writing the outbreak is still ongoing with new cases from 16 health zones and with fears that the disease will spread to larger cities in the area like Goma or accross borders. On the 17th of July the Director General of the WHO decleared the Ebola outbreak a Public Health Emergency of International Concern [15].

1.2 Modelling of Ebola

A large number of different mathematical models have been proposed for modelling Ebola, see e.g [1, 16]. The models can be divided into categories based on the structure of the models, mechanistic, semi-mechanistic, phenomenological and hybrid models. Mechanistic models are based on a specified mechanism for disease transmission and includes standard compartmental models while phenomenological models do not include any mechanism for disease transmission. An example of a phenomenological model would be an ARIMA model for the incidence. A semi-mechanistic model include some mechanisitc asumptions, but not a full model for disease transmission.

The RAPID Ebola Forcasting challeng in 2018 [16] presented a range of different scenarios of an ebola outbreak that was similar to the west african outbreak and invited different groups to submitt forecasts and compared them. They found that for short-term forecasting was not related to model complexity and that "light" non-parametric models were able to do well. The more complex mechanistic models would on the otherhand be better suited to understand the effects of interventions.

In this thesis we will present a semi-mechanisitc model that includes some mechanisitc assumptions about serial intervals and forces of infection combined with flexible time-series methods. The aim is a flexible model with parameters that are easily interpretable.

2 Methods

2.1 Data

We will use daily incidence data from the North Kivu Ebola outbreak as reported by the Ministry of Health in Congo and distributed via the humanitarian data exchange before the 1st of September 2019 [**?**]. We will use the incidence of confimed cases at the national and at the health-zone level. We use confirmed cases so that estimates of the reproduction number and other epidemiological parameters correspond only to Ebola and not Ebola and Ebola-like illnesess. Due to the nature of the outbreak and the nature of the data some confirmed cases are later found to not be Ebola. This can lead to days with negative incidence, we have chosen to set any negative incidence to zero. Data are missing for some days, for these days we lineraly interpolate the incidence.

2.2 Model

We consider a model where the daily incidence, I_t follows a modified branching process. Similar models have been considered in [17, 18, 19] and have been used to model Ebola during the 2014-2016 Ebola outbreak in Wester Africa [**?**, 20]. In this class of models each

infectious person gives rise to ν new infections, where ν is a random variable distributed with an offspring distribution with an expected value given by the reproduction number R. We use the serial interval to model the time between each generation of infections. This gives a process where the expected number of new cases at time t is given by the force of infection λ_t which is a product of previous incidence weighted by the serial interval w_τ and the instaneous reproduction number R_t.

$$E(I_t) = \lambda_t = R_t \sum_{s=1}^{t-1} I_s w_{t-s}$$

To fully specify the model we need to determine the probability distribution for I_t, the serial interval and the reproduction number as a function of time. For the serial interval we will use a gamma-distribution with mean 15.3 days and standard deviation of 9.3 days as fitted to data from the West-Africa Ebola outbreak [**?**]. Our general approach will be to use a few different spesifications for the I_t probability distribution and for estimating the time-varying reproduction number and then assess which model gives the best fit to the data.

2.2.1 Offspring distribution

The offspring distribution gives us the distribution of the number new infections from each infected person. By definition the expected value of this distribution is the reproduction number. The offspring distribution is a discrete probability distribution over the non-negative integers. The simplest such distribution is the poisson distribution, it is given by

$$P(X = k) = \exp -\lambda \frac{\lambda^k}{k!},$$

with mean and variance given by λ. This distribution implies that the number of new infections over a time interval is described by a constant rate where the chance of a new infection in each small sub-interval is independent.

For a number of diseases it has been shown that the offspring distribution has larger variance than that given by the poisson distribution and has so called superspreaders [18]. One common way of modelling this over-dispersed distribution is by the negative binomial distribution. The negative binomial distribution describes a process where we have a series of indepdent chances to infect a new interval each with probabilty p, where the process continues until we have had r infection chances without an infection. The distribution is given by

$$P(X = k) = \binom{k + r - 1}{k} (1 - p)^r p^k,$$

with $E(X) = \frac{pr}{1-p}$ and $Var(X) = \frac{pr}{(1-p)^2}$. We will use a parameterisation of the negative binomial distribution where we use the mean, μ and the dispersion parameter k. In this formulation the variance is given by $\mu(1 + \frac{1}{k})$. For $k- > \infty$ we get a poisson ditribution. The smaller k is the more the outbreak is dominated by a few super-spreaders and the larger k is the more similar the impact of each infected person is. For SARS it has been

found that $k = 0.16$[18]. For the Ebola outbreak in West Africa they found $k = 0.53$ using conservative assumptions and data from the network of infections [20]. The different offspring distributions ca be seen in Figure 1

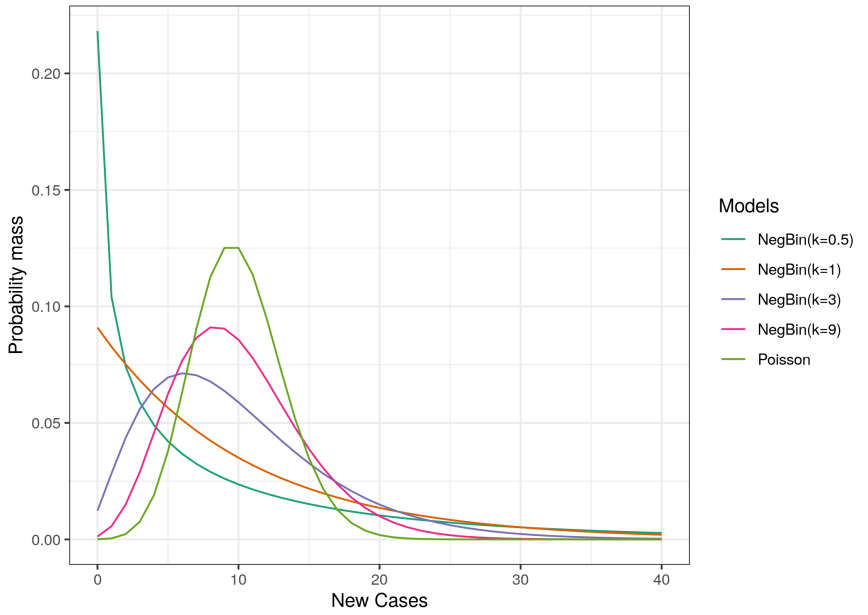

Figure 1: Poisson and negative binomial offspring distirubtions with a mean of 10.

The distribution for I_t would be given by the sum of the offspring distributions for each infected person (weighted by the serial distribution). For both the poisson and negative binomial distribution the sum of independent distriubtions will give back the same distribution with an expected value given by the sum of the expected values. For the negative binomial distribution the dispersion parameter k will remain the same.

We will investigate models with offspring distributions based both on the poisson distribution and the negative binomial distribution to assess which models fit the current outbreak better.

2.2.2 Reproduction number

The final ingredient to completely specify the dynamics of the model is the evolution of the reproduction number with time. Depending on the functional form of R_t, the model can fit a large range of possible epidemic behaviours.

It would be possible to specify a complete model for R_t analytically or otherwise, but in this thesis we will instead estimate R_t from the existing data and use these values to predict the future evolution of R_t. Since the focus of the current study is to provide a flexible framework for probabilistic prediction of disease outbreaks, this appraoch is suitable.

To estimate the reproduction number from the historical incidence data we use the method developed in [17]. If the reproduction number is estimated daily it is likely to varry too much from day to day in a manner that it is unrelastic. Therefore this method averages over the last 7 days to get more stable estimates. A baysian procedure is used to

estimate both the best fit value and the uncertainty of the estimate. We use the R-package EpiEstim [21] to estimate the reproduction number using a parametric gamma distribution for the serial interval with a mean of 15.3 days and a standard devitaion of 9.3 days [**?**]

Once we have calculated the historical values of R_t we can use them to provide an estimate of $R_t$moving forward that can be used for predictions. We will use two different procedures to predict the reproduction number. The first method is a very simple method were we assume that reproduction number remains constant from the last historical value. We use the uncertainties given by the method in [17] to provide estimates of the uncertainty of this estimate.

The second approch to predict the reproduction number is based on baysian structural time series fitted to the historical values of R. We use model with a semi-local linear trend to allow the estimation of a trend in the recent data. To ensure that predicted values of R are between 0 and 15 we fit the time series on a transfomed scale:

$$r^* = log\left(\frac{R}{15-R}\right)$$

We use the R-package BSTS [22] to fit the basysian structural time series. The model we use is specified as follows

$$r^*_{t+1} = r^*_t + \delta_t + \epsilon_t, \epsilon_t \sim N(0, \sigma_\mu),$$
$$\delta_{t+1} = D + \phi(\delta_t - D) + \eta_t, \eta_t \sim N(0, \sigma_\delta).$$

δ_t is the semi-local trend that we model as an AR(1) process that can oscilate around a level D. Inverse gamma-priors are used for the standar deviation parameters σ_μ and σ_δ, a gaussian prior on D and a $N(0, 0.1)$ prior for ϕ. The ϕ parameter determines how much the trend behaves as a random-walk. For $\phi = 1$ the trend follows a random walk, while for $\phi = 0$ the trend is just constant with some noice. We use a prior for small values of ϕ to keep the model for having very rapid growth in the variance of r^* that would be unphysical.

A Markow Chain Monte Carlo (MCMC) algorithm is used to estimate the parameters in the model which then allows us to predict future values of $r*$ with uncertainties, we then transform back to the R.

2.2.3 Simulating from the model

Once we have specified our model by specifying the offspring distribution and the method for forecasting R_t we can use the model to generate probabilistic forecasts. If we want to generate a forecast for I_{t+1} we first use all the data up until time t to estimte R_t and potentially fit the time series model to those values. Our probabelistic forecast will be based on sampling possible outcomes to generate a distribution of outcomes. We therefore first sample a value for R_{t+1} from our model, then we combin this with the historical incidence data to calculate λ_{t+1}. We then sample I_t from the specified offspring distribution. If we want to forecast over multiple time-steps we follow the same procedure by sampling values for the reproduction number. When calculating λ_{t+2} we use the sampled value for I_{t+1} together with the historical data I_s for $s \leq t$.

2.3 Assessing probabilistic forecasts

The aim of probabilistic forecasts is to predict both the correct average value and an appropriate uncertainty. Therefore it is not sufficient to only use metrics that depend on a point estimate, for example the Root Mean Square Error. We will follow the paradigm of maximizing sharpness of the predictive distribution subject to calibration [23]. In addition we will consider proper scoring rules for comparing probability ditributions. We follow the approach taken in [6], where probabilistic forecasts for the West African ebola outbreak were assessed using similar methods.

A model is calibrated if the uncertainties are accurate. For example if we predict that it will rain with 60% and we find that over time it does rain 60% of days where we predicted a 60% chance of rain, the model would be well calibrated. Mathematically, if we assume that real disribution of outcomes in nature is given by a cumulative density function G_t and our model predicts a cummulative density function F_t, we say that the forecast is ideal and perfectly calibrated if $F_t = G_t$. To assess calibration we will use a randomised Probability Integral Transformation (PIT) [24]. We calculate

$$u_t = F_t(k_t) + \nu(F_t(k_t) - F_t(k_t - 1)),$$

where k_t is the observed value at time, t and ν is a standard uniform random variable. If the prediction is ideal, the u_t will be distributed as a standard uniform distribution. We can then use the Anderson-Darling test of uniformity (goftest [25]) to assess if we can reject that the models are calibrated. Important to note that uniform PIT is a nescessary, but not suffcient condition for an ideal forecast. In addition to assessing calibration, the PIT histogram can tell us if the forcast is under or overdispersed. If the forcast is too dispersed the PIT values are likely to cluster in the centre of the PIT histogram, while if the forcast is underdispersed they are likely to clusteralong the edges of th histogram. We use a simple measure of centrality, which is equal to the fraction of u_t values that are between 0.25 and 0.75 as a way to assess if the forecasts are under or overdispersed if they are not calibrated.

$$\text{centrality} = \frac{N(0.25 < u_t < 0.75}{N} - 0.5$$

When the centrality scores is less than 0, most of the PIT values or outside of central region suggesting that the forecasts are underestimating the real uncertainty. If the centrality score is larger than 0 then the PIT scores are mainly in the central region and this indicates that the forecasts are overestimating the amount of uncertainty.

For both the test for uniformity and centrality we repeat the calculations 10 times and take averages to average out the effect of the randomness in the definition of u_t.

Sharpness is defined as the range of values in the forecast. The sharper a forecast, the more certain we are of predicted value. Sharpness depends only on the forecast and not on the observed values. We will use the normalised absolute devitation about the median of y to quantify sharpness:

$$S_t(F_t) = \frac{1}{0.675}\text{median}(|y - median(y)),$$

the normalisation factor means that S_t is equal to the standard deviation if F_t is normal.

It is also of importance to assess the bias of the forecast. Are we more likely to predict to large or too smal values? We will qunatify bias as

$$B_t(F_t, k_t) = 1 - (F_t(k_t) - F_t(k_t - 1)).$$

If $B_t = 0$ half the probability mass is above and half below the observed value, and the the forecast is unbiassed. B_t is between -1 and 1, with both extreme values signifying a completely biased forecast.

Proper scoring rules have been developed to rank forecasts. They combined calibration and sharpness and give a consistent ranking of forecasts. We will use the the contineously ranked probabilty score(CRPS) and the Dawid-Sebastiani score (DSS) as implemented in the scoringRules package [26]. The CRPS score is given by

$$CRPS(F_t, k_t) = \int_R (F_t(z) - \mathbb{1}k_t \leq z)^2 dz,$$

and the DSS only depens on the mean, μ_p and standard deviation, σ_p of the predictive distribution

$$DSS(F_t, k_t) = \left(\frac{k_t - \mu_p}{\sigma_p}\right)^2 + 2\log\sigma_p.$$

The DSS allows an intuitive understanding of the proper scoring rules. The first term tells us about the calibration of the predictions and the second term gives information about the sharpness. For our models we will only have samples from the predictive distribution. To calculate the CRPS a kernel density estimate is used to estimate F_t, for the DSS we use the mean and standard deviation of the sample.

2.4 Implementation

The models were implemented in the R programming langauge [27] and is available open source at http://github.com/gulfa/msc_ebola. We will consider four differrent models to assess which model fits the data best. The models are:

1. Model 1 (Poisson Latest): Constant reproduction number and poisson offspring distribution

2. Model 2 (NegBin Latest): Constant reproduction number and negative binomial offspring distribution

3. Model 3 (Poisson Semilocal): Varrying eproduction number and poissonoffspring distribution

4. Model 4 (NegBin Semilocal): Varrying reproduction number and negative binomial offspring distribution

For the dispersion parameter k for the negative binomial models we fit a value for the simple negativebinomial model by minimising the continous ranked probability score for the one day ahead predictions for the model on the level of the whole outbreak.

We will assess how well the models work both for the entire epidemic and for each health zone. To evalute a model we will estimate the calibration, sharpness, bias, log score and CRPS for forecasts of 1, 7, 14, 21 and 28 days ahead. To do this we start **check** 16 days after the start of the epidemic in the location and calculate the d ahead prediction for all historically available data. For the calibration we use all the values to assess if they are normally distributed, while for all the other metrics we average them over all the time steps. 16 days was chosen as the start as this is when the method for calculatng R_t can give somehat reliable values [17].

3 Results

From the start of the outbreak until the 31st of August 2019 there has been 2,926 confirmed ebola cases and 1926 confirmed ebola deaths. Figure 2a shows the weekly number of cases and Figure 2b the total number of cases from each Health Zone. From Figure 2a and the estimte of the instantaneous reproduction number in Figure **??** we can see the evolution of the outbreak. After the initial period were there were no daily surveillance, there was an increase in cases from October 2018 with a large reproduction number, followed a more varied period where the reproduction number varied around 1. From March 2019 the number of cases per week increased signficantly, with a continuing large number of cases in June and July even if the reproduction number seems to decrease. From the epi-curve there seems to a connection between the peaks and the large increases in specific health zones. So that pattern is in part driven by introduction or reintroduciton to individual health zones.

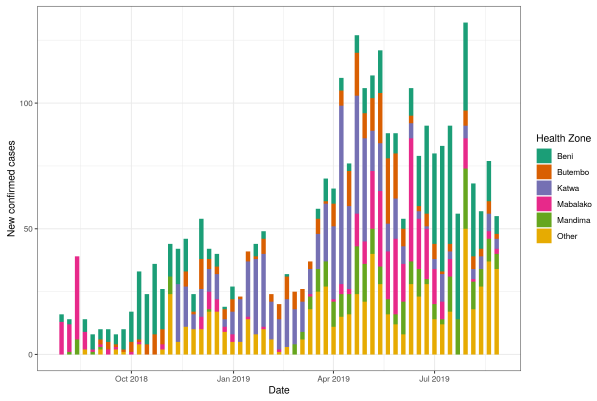

(a) Number of new confirmed cases by week in the health zones with the most Ebola Cases

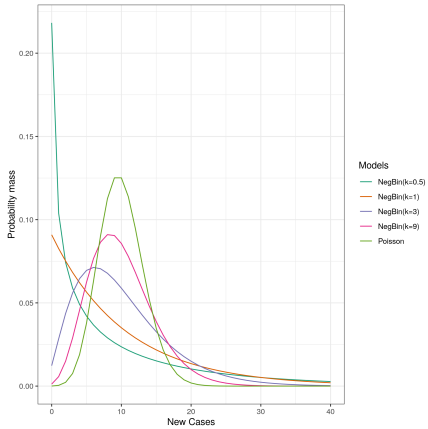

(b) Total number of confirmed cases by Health Zone

3.1 National level

We first found that the dispersion parameter that gives the smallest CRPS score for one day ahead predictions for the negative binomial models was k=8. Morevariance than a poisson distribution, but much less than found in previous Ebola outbreaks as discussed above.

On the level of the whole outbreak, the score for our four models for different forecasting horizons can be seen in Table 1.The evolution of the score can also be seen in Figure 3

model	horizon	sharpness	bias	crps	dss	centrality	calibration
Negative Binomial Semilocal	1	4.08	-0.66	1.87	3.30	0.04	0.19
Negative Binomial Latest	1	4.14	-0.66	1.82	3.26	0.06	0.19
Poisson Semilocal	1	2.93	-0.66	1.87	3.32	-0.08	0.00
Poisson Latest	1	2.97	-0.66	1.82	3.24	-0.08	0.00
Negative Binomial Semilocal	7	4.83	-0.67	1.80	3.41	0.17	0.00
Negative Binomial Latest	7	4.33	-0.67	2.36	3.94	-0.04	0.00
Poisson Semilocal	7	4.19	-0.67	1.72	3.23	0.09	0.01
Poisson Latest	7	3.08	-0.67	2.47	4.31	-0.14	0.00
Negative Binomial Semilocal	14	5.98	-0.68	2.56	4.62	0.13	0.00
Negative Binomial Latest	14	4.62	-0.68	2.82	4.74	-0.09	0.00
Poisson Semilocal	14	5.78	-0.68	2.52	4.54	0.10	0.00
Poisson Latest	14	3.28	-0.68	2.99	5.32	-0.21	0.00
Negative Binomial Semilocal	21	7.55	-0.68	3.24	5.69	0.15	0.00
Negative Binomial Latest	21	5.12	-0.68	4.07	5.57	-0.18	0.00
Poisson Semilocal	21	7.67	-0.68	3.26	5.88	0.15	0.00
Poisson Latest	21	3.53	-0.68	4.54	6.85	-0.25	0.00
Negative Binomial Semilocal	28	9.14	-0.69	4.77	7.43	0.17	0.00
Negative Binomial Latest	28	5.87	-0.69	5.30	7.38	-0.21	0.00
Poisson Semilocal	28	9.64	-0.69	4.89	7.12	0.16	0.00
Poisson Latest	28	3.88	-0.69	6.00	9.08	-0.28	0.00

Table 1: Model evaluations for predictions when all the models are fitted on the combined data from all the health zones.

Together they show that for next day forecast, the negative binomial offspring distirbution is needed for a calibrated forecast. The negative binomial distribution is clearly needed for a calibrated forecast even for one day ahead predictions. For longer forecasting horizons the poisson distribution with the semilocal time series prediction for R_t is the best model and is calibrated out to about 12 days. From the centrality scores, we can see that both the models with time series are overestimating the dispersion and the negative binomial model more so than the poisson model. Based on the scoring rules the two time series models are signficantly better than the models without any evaluation in R_t.

To understand the local poisson model better we calculate 28 day forecasts every 50 days of the outbreak and compared those forecasted incidence values with observed values. This can be seen in Figure 4. In the same figure we also plot the estimated values of the reproduction number together with 28 day forecasts for the same model. We see reasonable predictions, especially in the short term. We also here see that the model probably overestimates the uncertainty in both the reproduction number and the incidence.

3.2 Health Zones

4 Discussion

Limitations The data source for the model is the cummulative number of cases by days. We calculate the incidence as the difference in cummulative cases. This data source has many disadvantages to for example having a line list of all cases. A line list would give a much better idea of the data of onset of disease, it would remove the problem with negative incidence rates after corrections and any problems with having to interpolate incidence rates.

It is a strength of the modelling approach that it can be used on less than ideal data to still give reasonable short-term forecasts. In outbreak situations having up-to-date linelists of cases can be difficult or impossible, but we would still like to give reasonable forecasts.

The model in it's current form has several limitations. The main limitation on the Health Zone level is that spread between health zones is not modelled. The model structure is flexible enough to easily allow the incroporation of an addition force of infection term that gives the force of infection from outside the health zone. There are multiple options for how to model the geographic dependence that woul all easily fit into our model structure, this includes spread from adjacent health zones, using a gravity model where the amount of spread between health zones is based on the populations or if available data on inter health-zone travel could be used. Without this spread term the model can not be used to forecast probabilities for the spread of Ebola to new health zonez. In addition the current way of estimating the time-varrying reproduction number requires at least 12 days of data, so we need at least 12 days of data in a health zone to be able to forecast.

5 Conclusions

References

[1] J.-P. Chretien, S. Riley, and D. B. George, "Mathematical modeling of the West Africa Ebola epidemic," *eLife*, vol. 4.

[2] A. Camacho, A. Kucharski, Y. Aki-Sawyerr, M. A. White, S. Flasche, M. Baguelin, T. Pollington, J. R. Carney, R. Glover, E. Smout, A. Tiffany, W. J. Edmunds, and S. Funk, "Temporal Changes in Ebola Transmission in Sierra Leone and Implications for Control Requirements: a Real-time Modelling Study," *PLoS Currents*, vol. 7, Feb. 2015.

[3] P.-Y. Kobres, J. P. Chretien, M. A. Johansson, J. Morgan, P.-Y. Whung, H. Mukundan, S. D. Valle, B. M. Forshey, T. M. Quandelacy, M. Biggerstaff, C. Viboud, and S. Pollett, "A systematic review and evaluation of Zika virus forecasting and prediction research during a public health emergency of international concern," *bioRxiv*, p. 634832, May 2019.

[4] J.-P. Chretien, D. George, J. Shaman, R. A. Chitale, and F. E. McKenzie, "Influenza Forecasting in Human Populations: A Scoping Review," *PLOS ONE*, vol. 9, p. e94130, Apr. 2014.

[5] C. Rivers, J.-P. Chretien, S. Riley, J. A. Pavlin, A. Woodward, D. Brett-Major, I. M. Berry, L. Morton, R. G. Jarman, M. Biggerstaff, M. A. Johansson, N. G. Reich, D. Meyer, M. R. Snyder, and S. Pollett, "Using outbreak science to strengthen the use of models during epidemics," *Nature Communications*, vol. 10, pp. 1–3, July 2019.

[6] S. Funk, A. Camacho, A. J. Kucharski, R. Lowe, R. M. Eggo, and W. J. Edmunds, "Assessing the performance of real-time epidemic forecasts: A case study of Ebola in the Western Area region of Sierra Leone, 2014-15," *PLOS Computational Biology*, vol. 15, p. e1006785, Feb. 2019.

[7] W. Wei and L. Held, "Calibration tests for count data," *TEST*, vol. 23, pp. 787–805, Dec. 2014.

[8] T. Gneiting, "Editorial: Probabilistic forecasting," *Journal of the Royal Statistical Society: Series A (Statistics in Society)*, vol. 171, no. 2, pp. 319–321, 2008.

[9] World Health Organization, "Ebola Outbreak in DRC 01: 7 August 2018," Aug. 2018.

[10] World Health Organisation, "Ebola Outbreak in DRC 09: 04 October 2018," Oct. 2018.

[11] World Health Organization, "Ebola Outbreak in DRC 16: 21 November 2018," Nov. 2018.

[12] World Health Organization, "Ebola Outbreak in DRC 38: 24 April 2019," Apr. 2019.

[13] W. H. Organization, "Preliminary results on the efficacy of rVSV-ZEBOV-GP Ebola vaccine using the ring vaccination strategy in the control of an Ebola outbreak in the Democratic Republic of the Congo: an example of integration of research into epidemic response.," tech. rep., Apr. 2019.

[14] National Institute of Allergy and Infectious Diseases, "Independent Monitoring Board Recommends Early Termination of Ebola Therapeutics Trial in DRC Because of Favorable Results with Two of Four Candidates," Aug. 2019.

[15] World Health Organization, "Ebola Outbreak in DRC 51: 23 July 2019," July 2019.

[16] C. Viboud, K. Sun, R. Gaffey, M. Ajelli, L. Fumanelli, S. Merler, Q. Zhang, G. Chowell, L. Simonsen, and A. Vespignani, "The RAPIDD Ebola Forecasting Challenge: Synthesis and Lessons Learnt," *Epidemics*, vol. 22, pp. 13–21, Mar. 2018.

[17] A. Cori, N. M. Ferguson, C. Fraser, and S. Cauchemez, "A new framework and software to estimate time-varying reproduction numbers during epidemics," *American Journal of Epidemiology*, vol. 178, pp. 1505–1512, Nov. 2013.

[18] J. O. Lloyd-Smith, S. J. Schreiber, P. E. Kopp, and W. M. Getz, "Superspreading and the effect of individual variation on disease emergence," *Nature*, vol. 438, p. 355, Nov. 2005.

[19] P. Nouvellet, A. Cori, T. Garske, I. M. Blake, I. Dorigatti, W. Hinsley, T. Jombart, H. L. Mills, G. Nedjati-Gilani, M. D. Van Kerkhove, C. Fraser, C. A. Donnelly, N. M. Ferguson, and S. Riley, "A simple approach to measure transmissibility and forecast incidence," *Epidemics*, vol. 22, pp. 29–35, Mar. 2018.

[20] International Ebola Response Team, J. Agua-Agum, A. Ariyarajah, B. Aylward, L. Bawo, P. Bilivogui, I. M. Blake, R. J. Brennan, A. Cawthorne, E. Cleary, P. Clement, R. Conteh, A. Cori, F. Dafae, B. Dahl, J.-M. Dangou, B. Diallo, C. A. Donnelly, I. Dorigatti, C. Dye, T. Eckmanns, M. Fallah, N. M. Ferguson, L. Fiebig, C. Fraser, T. Garske, L. Gonzalez, E. Hamblion, N. Hamid, S. Hersey, W. Hinsley, A. Jambei, T. Jombart, D. Kargbo, S. Keita, M. Kinzer, F. K. George, B. Godefroy, G. Gutierrez, N. Kannangarage, H. L. Mills, T. Moller, S. Meijers, Y. Mohamed, O. Morgan, G. Nedjati-Gilani, E. Newton, P. Nouvellet, T. Nyenswah, W. Perea, D. Perkins, S. Riley, G. Rodier, M. Rondy, M. Sagrado, C. Savulescu, I. J. Schafer, D. Schumacher, T. Seyler, A. Shah, M. D. Van Kerkhove, C. S. Wesseh, and Z. Yoti, "Exposure Patterns Driving Ebola Transmission in West Africa: A Retrospective Observational Study," *PLoS medicine*, vol. 13, p. e1002170, Nov. 2016.

[21] A. Cori, *EpiEstim: EpiEstim: a package to estimate time varying reproduction numbers from epidemic curves.* 2013.

[22] S. L. Scott, *bsts: Bayesian Structural Time Series.* 2019.

[23] T. Gneiting, F. Balabdaoui, and A. E. Raftery, "Probabilistic forecasts, calibration and sharpness," *Journal of the Royal Statistical Society: Series B (Statistical Methodology)*, vol. 69, no. 2, pp. 243–268, 2007.

[24] C. Czado, T. Gneiting, and L. Held, "Predictive Model Assessment for Count Data," *Biometrics*, vol. 65, no. 4, pp. 1254–1261, 2009.

[25] J. Faraway, G. Marsaglia, J. Marsaglia, and A. Baddeley, *goftest: Classical Goodness-of-Fit Tests for Univariate Distributions*. 2017.

[26] A. Jordan, F. Krueger, and S. Lerch, "Evaluating Probabilistic Forecasts with scoringRules," *Journal of Statistical Software*, 2018.

[27] R Core Team, *R: A Language and Environment for Statistical Computing*. Vienna, Austria: R Foundation for Statistical Computing, 2018.

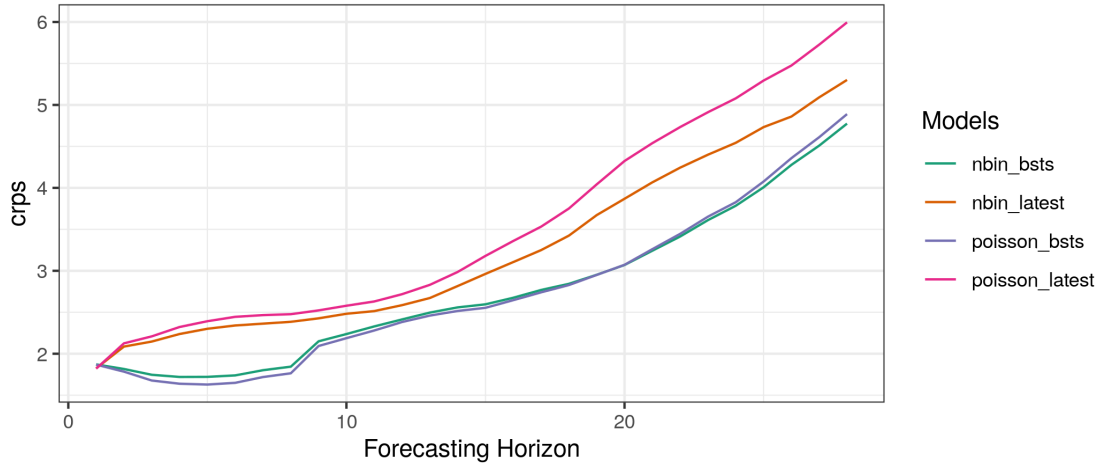

(a) Contineously Ranked Probability Score

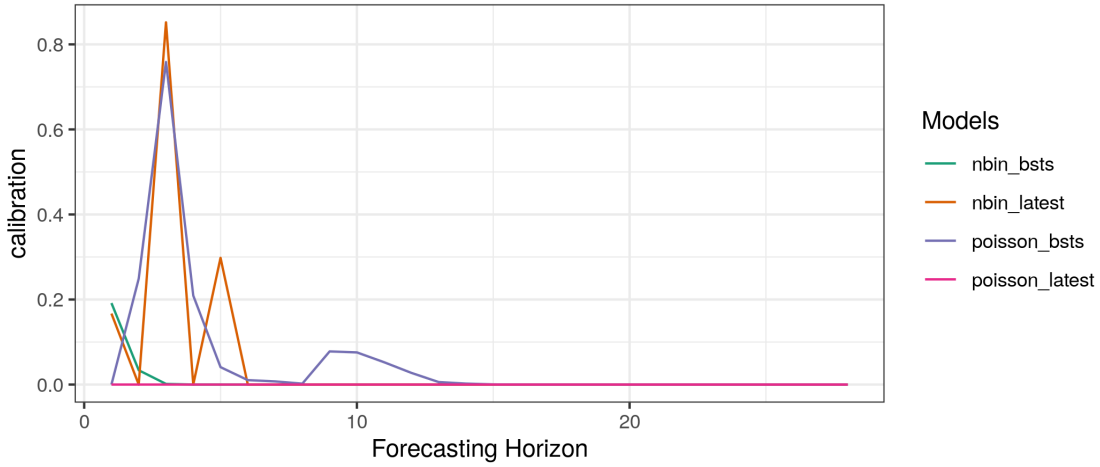

(b) Calibration p-value

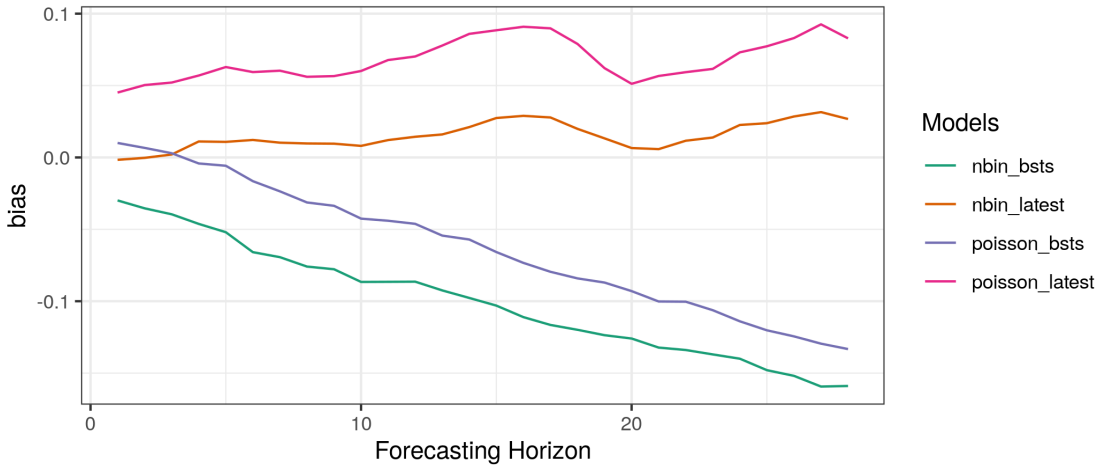

(c) Bias

Figure 3: Scores for the entire outbreak as a function of the forecasting horizon.

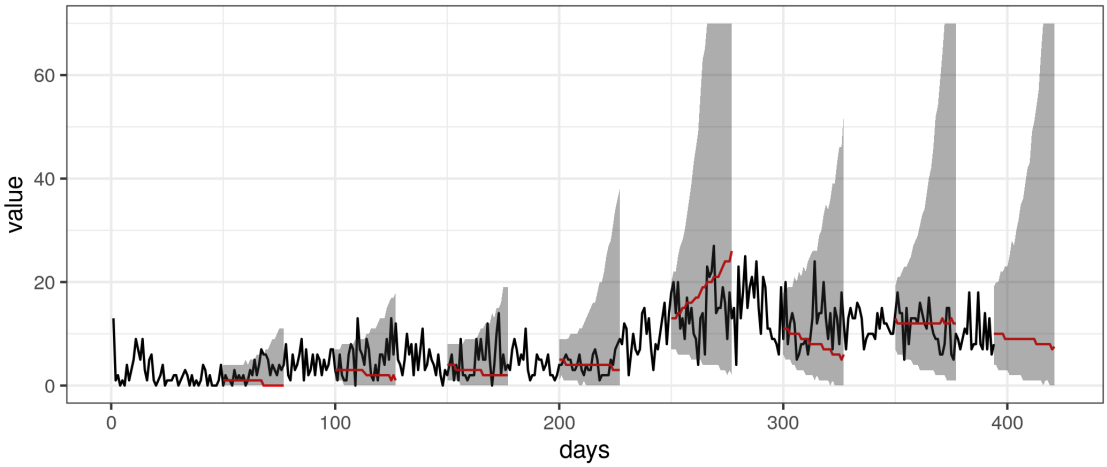

(a) Forecasted and predicted incidence for the semilocal poisson model

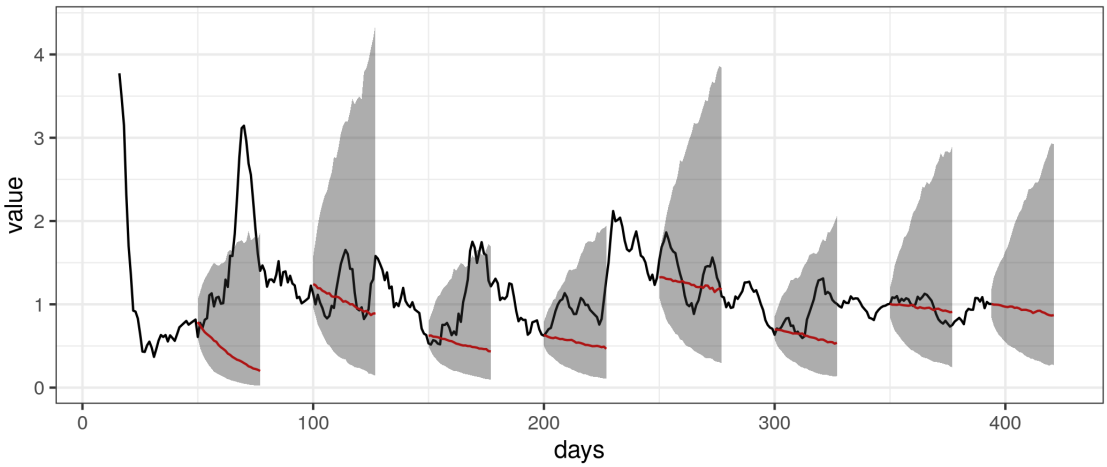

(b) Forecasted and predicted repreoduction numbers for the semilocal poisson model

Figure 4: Median forecast with 95% prediction intervals and observed values for incidence and reproduction number for the semilocal poisson model

.

Location	Largest Horizon	Best model	Cases
Kayna	28	NegBin Semilocal, Poisson Semilocal	22
Nyiragongo	28	NegBin Semilocal, Poisson Semilocal	3
Tchomia	28	NegBin Semilocal, Poisson Semilocal	2
Lolwa	26	NegBin Semilocal, NegBin Latest, Poisson Semilocal, Poisson Latest	3
Bunia	18	NegBin Semilocal	4
Mwenga	18	NegBin Semilocal, NegBin Latest, Poisson Semilocal, Poisson Latest	6
Alimbongo	13	NegBin Latest	5
national	9	Poisson Semilocal	2942
Kayina	7	NegBin Latest, Poisson Semilocal	10
Rwampara	6	NegBin Latest	8
Lubero	5	Poisson Semilocal	31
Butembo	3	NegBin Semilocal	279
Kyondo	3	NegBin Semilocal	22
Mabalako	3	NegBin Semilocal	371
Vuhovi	3	Poisson Semilocal	103
Beni	2	NegBin Semilocal, Poisson Semilocal	661
Biena	2	Poisson Latest	16
Musienene	2	NegBin Semilocal	84
Goma	NA	No calibrated model	1
Kalunguta	NA	No calibrated model	164
Katwa	NA	No calibrated model	647
Mangurujipa	NA	No calibrated model	20
Masereka	NA	No calibrated model	50
Mutwanga	NA	No calibrated model	31
Oicha	NA	No calibrated model	55
Pinga	NA	No calibrated model	1
Ariwara	NA	No calibrated model	1
Komanda	NA	No calibrated model	43
Mambasa	NA	No calibrated model	32
Mandima	NA	No calibrated model	264
Nyankunde	NA	No calibrated model	1
Rwampara (Bunia)	NA	No calibrated model	1

Table 2: For each health zone we show the best maximal forecasting horizon where we can not exclude calibration at the p=0.1 level. We also show which models could provide this calibrated forecast